INTERVENTIONAL RADIOLOGY
Official journal of the Japanese Society of Interventional Radiology and Asia Pacific Society of Cardiovascular and Interventional Radiology

REVIEW

Innovative Techniques for Image-guided Percutaneous Puncture: Navigating Complex Cases for Successful Outcomes

Taku Yasumoto, Koichi Yamada, Hakketsu Koh and Ryoong-Jin Oh

Department of Interventional Radiology, Miyakojima IGRT Clinic, Japan

Abstract:
This article emphasizes image-guided puncture, a common technique used by interventional radiologists. It focuses on ultrasound, fluoroscopy, computed tomography, and computed tomography fluoroscopy-guided procedures. While techniques vary, successful outcomes without complications still heavily rely on operators' skill and judgment. Operators need knowledge of needle characteristics and expert needle manipulation. Continual skill refinement through daily practice is essential, aiming maximum results with minimal invasiveness. This article examines challenging cases of percutaneous needle biopsy, biliary intervention, radiofrequency ablation, and percutaneous abscess drainage while referencing previous review articles and discusses how to succeed in these cases by employing various techniques and approaches in various image-guided procedures. This article aimed to provide interventional radiologists with a comprehensive and practical guide for enhancing their image-guided puncture techniques, ultimately leading to successful outcomes.

Keywords:
image-guided puncture, challenging case, CT fluoroscopy guidance, X-ray fluoroscopy guidance, computed tomography guidance

Interventional Radiology 2024; 9(3): 99-111
https://doi.org/10.22575/interventionalradiology.2024-0003
https://ir-journal.jp/

Introduction

Image-guided puncture is a minimally invasive and effective technique used for various procedures, such as percutaneous needle biopsy [1-3], abscess drainage [4, 5], percutaneous transhepatic biliary drainage (PTBD) [6-9], and ablation therapies including RFA [10-18]. Some review articles reported basic interventional techniques such as percutaneous needle biopsy, abscess drainage, PTBD, and RFA [1-6, 10-17]. However, there are no established guidelines for the optimal method for cases generally considered difficult, and the skill and judgment of the operator is critical. Furthermore, despite the generally safe nature of the procedure, a certain percentage of cases result in technical failures or major complications (**Table 1**) [1-18].

In general, interventional radiologists (IRists) heavily rely on diagnostic imaging equipment. However, the fundamental principle for IRists is to understand the type and characteristics of the needle or catheter and acquire the skill and delicacy necessary to manipulate these devices by hand. Continual improvement of these skills through daily practice is essential in achieving the best results with minimal invasion for the patient.

This article focuses on four major procedures: percutaneous needle biopsy, PTBD, RFA, and percutaneous abscess drainage, specifically highlighting innovative techniques for success in challenging puncture situations. These techniques have not been previously reported in review articles, aside from basic image-guided puncture. Our review will focus on various methods used under ultrasound guidance, X-ray fluoroscopy guidance, CT guidance, and CT fluoroscopy guidance.

Challenging Cases of Percutaneous Needle Biopsy

Percutaneous needle biopsy (PNB) is a procedure commonly performed in interventional radiology, with ultrasound (US) and CT being the primary imaging modalities used for guidance. Other uncommon imaging techniques, such as fluoroscopy, magnetic resonance imaging (MRI),

Corresponding author: Taku Yasumoto, yasumoto@solid.ocn.ne.jp
Received: January 29, 2024, Accepted: February 11, 2024, Advance Publication by J-STAGE: October 4, 2024

Table 1. Summary of Recent Studies of Image-Guided Percutaneous Puncture Procedures.

Author	Publication year	Study design	Procedure	Target organ or lesion	Clinical success rate [%]	Major AE rate [%]
Sheth et al. [1]	2020	Practice guidelines	Biopsy	Lung > 3 cm	93	1.0–4.1
				Lung 2–3 cm	96	
				Lung 1–2 cm	92–93	
				Lung < 1 cm	93	
Sheth et al. [1]	2020	Practice guidelines	Biopsy	Musculoskeletal/soft tissue	84	N.A.
				Musculoskeletal/sclerotic bone	74	
Lane et al. [2]	2008	Review	Biopsy	Kidney	79–98	0.3–3.8
Iguchi et al. [3]	2020	Review	Biopsy	Kidney	68–97	0.4–2.1
Sheth et al. [1]	2020	Practice guidelines	Biopsy	Liver	83–99	1.3
Dariushnia et al. [4]	2020	Practice guidelines	Drainage	Abscesses and abdominal fluid collection	62–100	0–15
Keeling et al. [5]	2008	Review	Drainage	Empyema and thoracic effusion	76–99	3–22
Devane et al. [6]	2020	Practice guidelines	PTBD	Dilated ducts	90–100	4.5–9.0
				Nondilated ducts	67–97	
Mahjoub et al. [7]	2016	Meta-analysis	PTBD	Preoperative biliary drainage	75.5	7.5
Dorcaratto et al. [8]	2018	Systematic review and meta-analysis	PTBD	Biliary drainage before pancreatoduodenectomy	N.A.	16
Shiina et al. [10]	2018	Review	RFA	HCC	*73–98	N.A.
Sato et al. [11]	2020	Review	RFA	HCC	N.A.	0.9–10.0
Tanis et al. [12]	2014	Prospective randomized phase III trial	RFA	Metastatic liver tumor	*86–94	N.A.
White et al. [13]	2007	Retrospective study	RFA	Metastatic liver tumor	*53–91	4
Matsui et al. [14]	2020	Review	RFA	Non-small cell lung cancer	*63–81	N.A.
Hiraki et al. [15]	2013	Review	RFA	Lung cancer	N.A.	6–29
Lyons et al. [16]	2015	Systematic review	RFA	Lung metastases	N.A.	0.5–8
Hasegawa et al. [17]	2020	Prospective multicenter study	RFA	Lung metastases < 2.8 cm	*89–91	1

Note-Data are based on pooled rates from review articles, systematic reviews with meta-analysis. In cases in which a systematic review was not available, individual studies with N > 50 were used in the calculation of rates.

AE, adverse event; N.A., not available; PTBD, percutaneous transhepatic biliary drainage; RFA, radiofrequency ablation; HCC, hepatocellular carcinoma; *Local control rate.

and PET-CT, may also be used. CT fluoroscopy, a real-time visualization technique, can reduce procedural time but can expose operators and patients to radiation doses [19]. Success in PNB is related to proper patient selection, preparation, and adequate procedural planning [20, 21].

A previous review article reported that the success rates of percutaneous biopsy range from 74% to 100%, with results varying by site [1]. In particular, a 74% lower success rate was reported for sclerotic bone lesions [1]. In difficult cases, familiarity with various methods that have been described to sample difficult-to-reach lesions is essential to minimize complications, for example, triangulation method for out-of-plane approach, angling of the CT gantry, injection of fluid or air to displace intervening structures, creative patient positioning, use of a curved needle (precurved or manually deformed), use of a needle with a blunt trocar, use of electromagnetic navigation systems, and use of abdominal compression to move the intervening structures [22-29].

Innovative percutaneous biopsy techniques

This article presents several cases of successful PNB under difficult situations in a manner not previously coherently reported, focusing on the innovative techniques used to achieve success (**Fig. 1**-**3**).

A case of left retroperitoneal mass adjacent to the left common iliac artery is shown (**Fig. 1**). CT-guided percutaneous biopsy with hydrodissection by using blunt-tip needle (HydroGuard®; Apriomed, Sweden) coaxially was successfully performed avoiding the vessels adjacent to the mass and the gastrointestinal tract along the puncture route. Blunt-tip needle is useful for percutaneous biopsy of hard-to-reach targets [30, 31].

Percutaneous biopsy of a mass invading into duplicated inferior vena cava was performed using CT fluorotic venography to prevent vascular damage (**Fig. 2**). When CT fluoroscopy alone does not clarify the positional relationship between the target and surrounding vascular anatomy, CT fluoroscopy-guided puncture with angiography, such as venography, is effective in this way.

We sometimes experience percutaneous biopsy of a difficult-to-diagnose tumor of the renal pelvis. Since the relationship of the renal pelvis tumor to the normal renal pelvis, renal parenchyma, and renal arteriovenous system is unclear on plain CT, biopsy using contrast-enhanced CT fluoroscopy allows for safe tissue collection from the tumor. A review article [2] by Lane et al. reported that a total success rate of greater than 90% is attainable using renal mass biopsy with standard histopathological analysis and that tech-

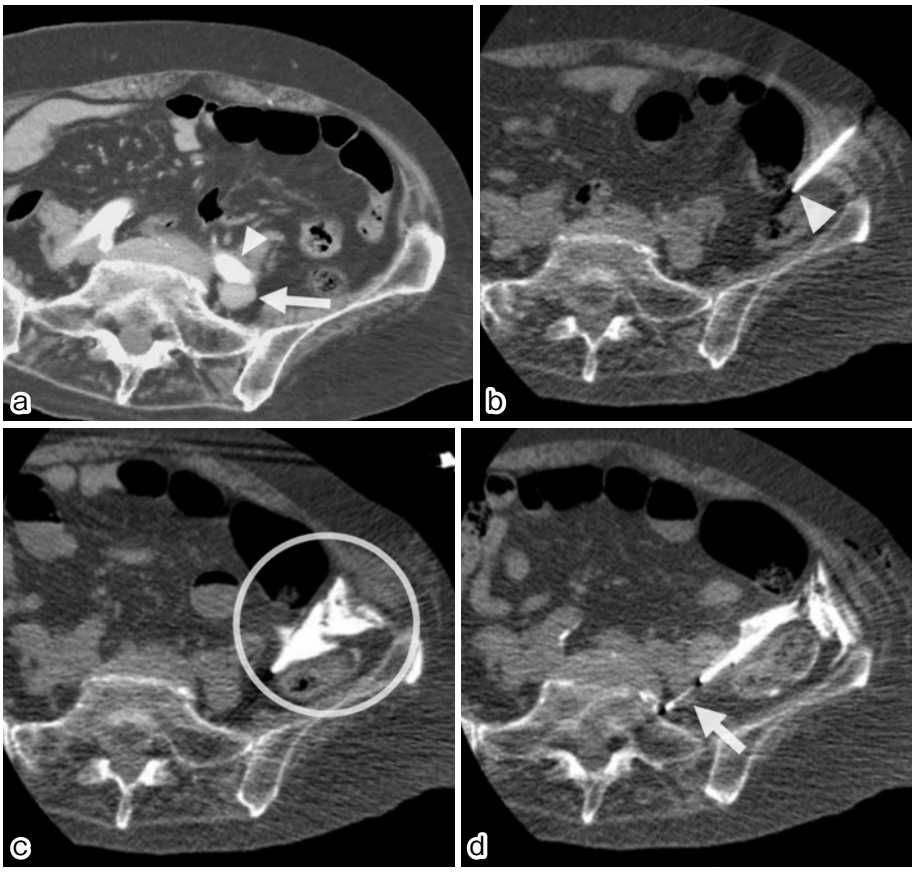

Figure 1. CT fluoroscopy-guided percutaneous needle biopsy after hydrodissection using blunt-tip needle for left retroperitoneal mass adjacent to left common iliac artery.
Enhanced CT reveals left retroperitoneal mass (a: arrow) adjacent to the left common iliac artery (a: arrowhead). Percutaneous biopsy from abdominal wall had risks of active bleeding and perforation of the digestive tract. So blunt-tip coaxial needle (SoftGuard®, AprioMed AB, Uppsala, Sweden) was advanced at first to avoid injury of the intestine (b, arrow head: the tip of the blunt-tip coaxial needle). After hydrodissection by injecting contrast medium diluted with 20x saline (c, circle), a percutaneous biopsy of the left retroperitoneal mass shadow was performed using an 18-G semi-automatic biopsy needle (d, arrow) in a coaxial needle.

nical failure (inability to obtain tissue to submit for diagnosis) occurred in 8.9% of percutaneous renal mass biopsies (range 0%-22%). Contrast-enhanced CT fluoroscopic-guided biopsies allow more samples to be taken, which may improve the diagnostic yield.

A case of percutaneous biopsy of an osteosclerotic lesion of the sternum using the ARROW OnControl® powered bone access system (Teleflex, Shavano Park, TX, USA) is presented (**Fig. 3**). OnControl® bone access system uses a drill function, which is more powerful and allows the needle to reach hard tissue more easily than a manual-type biopsy needle and is also more effective for inadequate bone sample can be taken, contributing to improved diagnostic performance. It has been reported that OnControl® bone access system decreases procedure time, reduces operator exposure, and significantly increases the median total specimen yield compared to a manual-type biopsy needle and is a device that directly improves the diagnostic yield of sclerotic bone biopsy [32, 33].

These cases highlight the importance of technical skill and experience in percutaneous biopsy procedures and demonstrate the potential benefits of employing clinically practical unconventional approaches to achieve success in challenging cases.

Challenging Cases of Biliary Intervention

A previous review article reported an overall procedure-related morbidity rate of 44.3% (82 out of 185) in the endoscopic retrograde biliary drainage (ERBD) group and 26.5% (39 out of 147) in the PTBD group [4]. This analysis showed that the overall procedure-related morbidity rate was significantly higher in the ERBD group (odds ratio (OR), 2.23; 95% confidence interval (CI), 1.39-3.57; P = .0009) than in the PTBD group. Devane et al. reported that the success rate of percutaneous transhepatic cholangiography and biliary drainage for dilated and nondilated bile ducts was 97.6% and 86.9%, respectively. The clinical success rate was 85.5% and 69.8% for dilated and nondilated ducts, respectively [6].

Percutaneous puncture of nondilated bile ducts is commonly considered challenging. Various techniques, such as

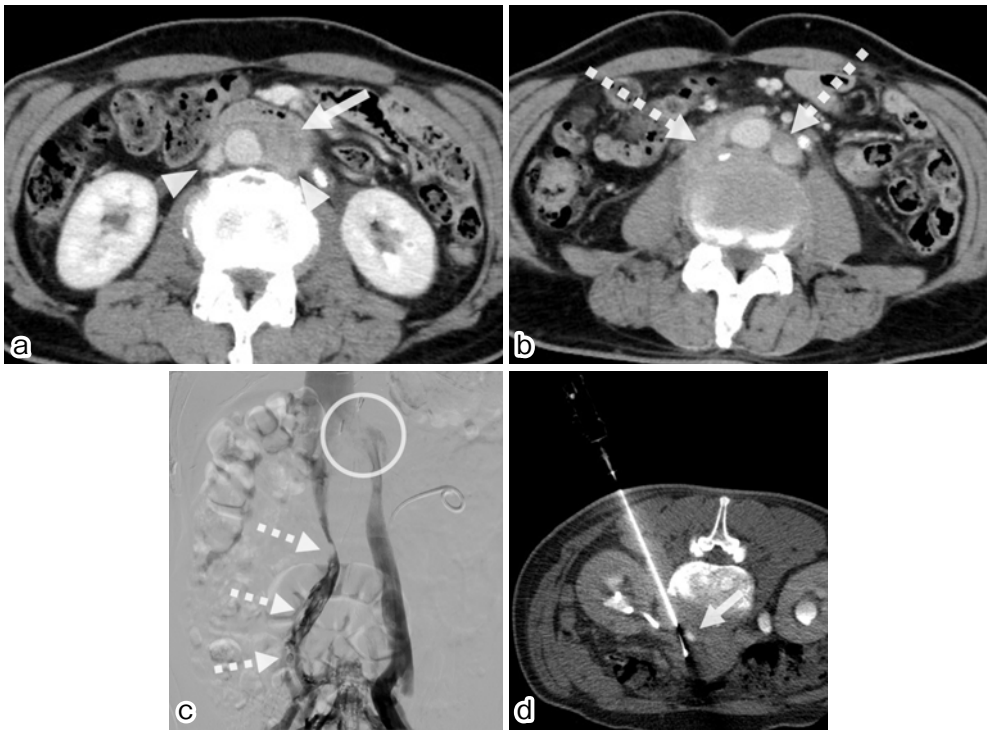

Figure 2. CT fluorotic venography-guided percutaneous needle biopsy for left retroperitoneal tumor invading into duplicated inferior vena cava complicating ureteral carcinoma.
In a case involving a left ureteral tumor with a duplicated inferior vena cava (a: arrowheads), contrast-enhanced CT revealed that the retroperitoneal tumor (a: arrow) appeared to invade the duplicated inferior vena cava at the caudal level (b: dotted arrows). Venography of the right-sided inferior vena cava, from the right femoral vein, revealed collateral vessels transporting blood from the left inferior vena cava obstructed by the retroperitoneal tumor (c: circle) due to significant stenosis of the right inferior vena cava (c: dotted arrows). To obtain a biopsy of the retroperitoneal tumor while avoiding the left inferior vena cava, the procedure was conducted under CT fluoroscopy with venography from the left-sided inferior vena cava (d, arrow: left-sided inferior vena cava). Fortunately, there were no technical complications, including bleeding or injury to the vena cava. Pathological analysis confirmed that the tumor was metastasis from ureteral carcinoma.

fluoroscopic puncture [34, 35], Gleason sheath puncture, cystic ductal approach from percutaneous transhepatic gallbladder biliary drainage (PTGBD) [36], percutaneous balloon puncture [34], CT fluoroscopy-guided puncture [34], and drip infusion cholangiography (DIC)-CT fluoroscopy-guided puncture [34], have been reported. Although each method is useful, we present a challenging case that could have been treated with a different technique but was successfully managed using a combination of these methods (**Fig. 4**).

CT fluoroscopy-guided puncture for emphysematous biliary perforation

CT fluoroscopy-guided puncture can be a valuable technique for challenging cases of emphysematous biliary perforation. For instance, a woman in her 60s who had previously undergone pancreaticoduodenectomy for duodenal carcinoid tumor developed a refractory biliary fistula with biliary emphysema (**Fig. 4**). Due to the difficulty in visualizing the bile duct with US, a puncture was performed under CT fluoroscopy, targeting a small air pocket observed within the bile duct. Subsequently, the catheter beyond the biliary fistula was successfully redirected to create an internal fistula. A 7-French (Fr) pigtail catheter with a side hole was inserted to establish both internal and external fistulas, gradually mitigating the severity of the biliary fistula.

The use of an 18-Gauge (G) PTBD needle is the key to the technique of CT fluoroscopy-guided biliary puncture for emphysematous bile duct. Upon entering the hepatic parenchyma and encountering the air within the bile duct, there should be a slight decrease in resistance, which can be sensed at the fingertips. Even if this sensation is not clearly felt, it serves as an indicator for accurate positioning in the air, as movement of the air on CT fluoroscopy can be instantly observed. When considering the removal of the inner needle, advancing the J-shaped spring guidewire (GW) about 2 mm toward the central side from the point where resistance was felt can ensure smooth advancement, all while being mindful of the short distance from the outer cylinder.

This technique necessitates precision in moving the CT fluoroscopy screen bed or gantry in millimeter increments to keep the tip of the GW in sight. In such cases, employing the one-person method is preferable over the two-person method, with the operator making fine the Z-axis adjust-

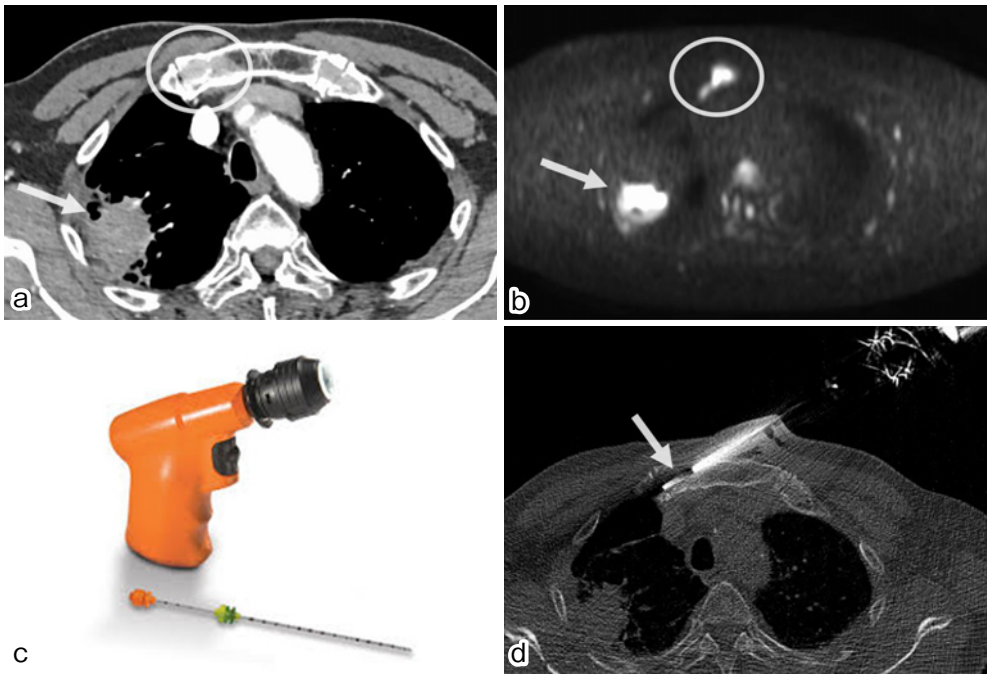

Figure 3. Percutaneous biopsy of an osteosclerotic lesion located on the right side of the sternum, using the OnControl® powered bone access system.
Dynamic CT images (a: arterial phase) reveal the presence of primary lung cancer in the right upper lobe of the right lung, along with osteoid changes on the right side of the sternum (arrow: primary lung cancer, circle: osteosclerotic changes on the right side of the sternum). DWI of the MRI exhibits a high signal consistent with primary lung cancer and an osteosclerotic lesion on the right side of the sternum (b). The power driver of the OnControl® and the puncture needle are shown (c). A percutaneous biopsy was successfully performed with easy access to the sternal osteosclerotic lesion using OnControl® under CT fluoroscopic guidance (d, arrow: biopsy needle tip). Pathological results confirmed bone metastasis from primary lung cancer, leading to the administration of systemic chemotherapy.

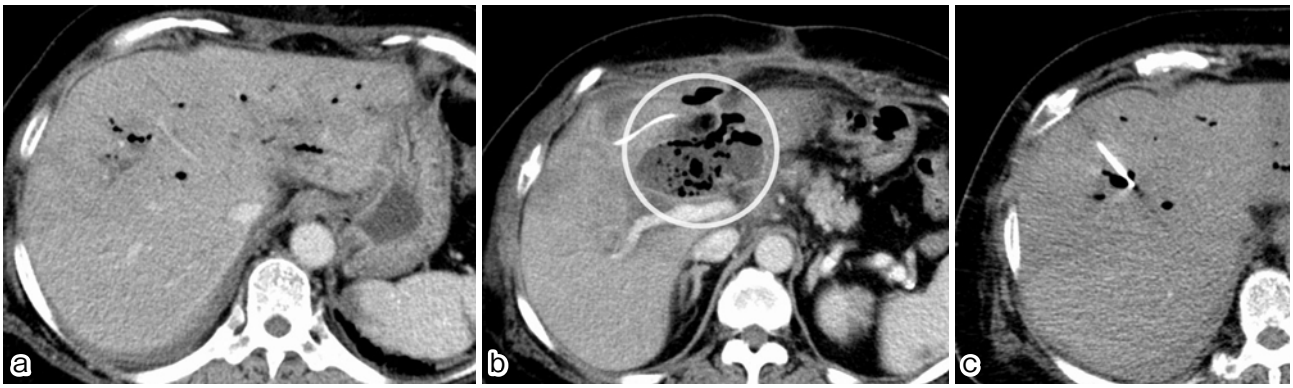

Figure 4. CT fluoroscopy-guided air puncture for pneumobilia and refractory bile leakage after pancreaticoduodenectomy.
Enhanced CT reveals pneumobilia (air within the biliary tree of the liver) (a) and refractory bile leakage and abscess (b: circle) near the choledochojejunostomy after pancreaticoduodenectomy for a carcinoid tumor of the duodenum. CT-guided puncture was performed from caudal to cranial direction for the nondilated bile duct filled with air regurgitation from the jejunum (pneumobilia) (c).

ments using their non-puncturing hand. Once the GW is properly positioned in the bile duct with the tip forming the correct J shape, the drainage tube can be guided using regular fluoroscopy.

Even in the absence of intrahepatic bile duct dilation, proficiency in the technique of CT fluoroscopy-guided puncture can help achieve the procedural endpoint when dealing with biliary emphysema. In addition, a preoperative contrast-enhanced CT examination should be conducted to identify existing structures, including surrounding normal elements such as vessels, pulmonary parenchyma, or intestines.

X-ray fluoroscopy-guided puncture for emphysematous bile duct

This case involves a patient with biliary emphysema resulting from metallic stent placement for cholangiocarci-

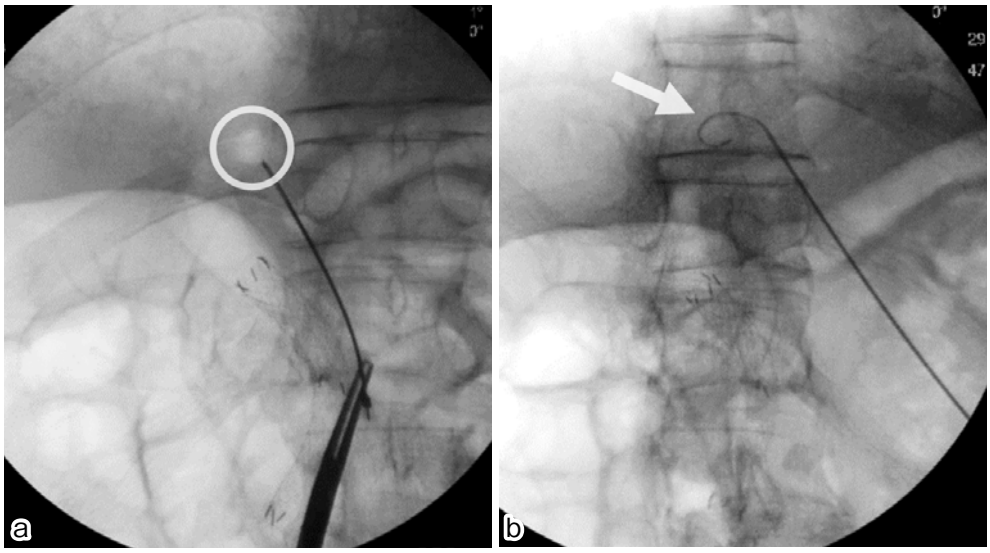

Figure 5. X-ray-guided air puncture (PTBD for pneumobilia).
While gripping the PTBD needle with forceps, the air in the bile duct is visualized under X-ray fluoroscopy guidance (a). The guidewire (arrow) is passed through the mantle and advanced to the left hepatic duct (b). The air becomes obscured due to the effect of accurate puncture.

noma, which had led to cholangitis due to stent obstruction. Due to the presence of gastrointestinal gas, the liver could not be visualized using US. Instead, the dilated emphysematous bile duct was identified using X-ray fluoroscopy. A puncture was performed under fluoroscopy guidance to access an air image consistent with the left hepatic duct (**Fig. 5**).

However, it is essential to master the technique of accurately inserting the needle tip in a direction consistent with the target while rotating the C-arm or flat panel as needed, regardless of the presence or absence of biliary emphysema when performing fluoroscopic punctures of the bile ducts. In this case, we found that having one operator who can fine-tune the needle tip to the target is more effective than having two. It is crucial to master the one-operator technique (i.e., grasping the needle with one hand and rotating the C-arm with the other hand). We believe that this technique will enable operators to handle various other difficult puncture cases, but more cases need to be accumulated. Since the technique requires skill, it is essential to hold the puncture needle with forceps to protect the operator from radiation exposure.

Therefore, when both CT- and US-guided punctures are difficult, X-ray fluoroscopy-guided puncture may be a viable option. It is important to accumulate more cases to refine this technique.

Challenging Cases of RFA

IRists typically employ ablation therapy for malignant liver tumors situated in proximity to the gastrointestinal tract or diaphragm. This procedure often involves CT fluoroscopy techniques such as the use of artificial ascites [30, 31], hydrodissection, hyaluronic acid puncture [32], or balloon dissection [33]. It has been reported that unlike hepatocellular carcinoma [10], RFA for metastatic liver tumors showed local recurrence in 6%-55% of patients during a follow-up period of 17-74 months, which is not a favorable result [41-47]. Yamakado et al. reported that RFA for metastatic liver tumor from colorectal cancer performed under CT fluoroscopy with injection of degradable starch microspheres (DSM) (Spherex; Yakult Co., Ltd., Tokyo, Japan) resulted in good ablative margin and that the local control rate was 92.1% [46]. We previously reported a case in which we achieved a complete response in a patient with liver metastases from gastric cancer using this approach [47]. This suggests that RFA with controlled blood flow is effective not only for hepatocellular carcinoma but also for metastatic tumors.

However, in cases involving very hypovascular metastatic liver tumors, RFA with DSM may pose challenges due to the unclear contrast effect at the tumor margins. In such situations, it has been proven that RFA with CT during arterial portography is a useful alternative [48]. This technique requires a relatively large amount of contrast medium. Another approach is to inject a mixture of non-ionic iodine contrast medium (Iopamiron 300, 100 ml, Bayer Healthcare, Osaka, Japan) and iodized oil (Lipiodol Ultra Fluid® (LPD), Laboratories Gerber, Aulnay-sous-Bois, France) into the subsegment containing the tumor. Subsequently, the metastatic tumor can be punctured under CT guidance, taking advantage of the contrast deficiency.

Innovative percutaneous radiofrequency ablation techniques

This case involved a postoperative liver metastasis from gastric cancer with a hypovascular metastasis located in the left anterior and dorsal segment (S3). This tumor was adjacent to the residual stomach and the left gastric artery (**Fig. 6**). Conducting a general hydrodissection was challenging

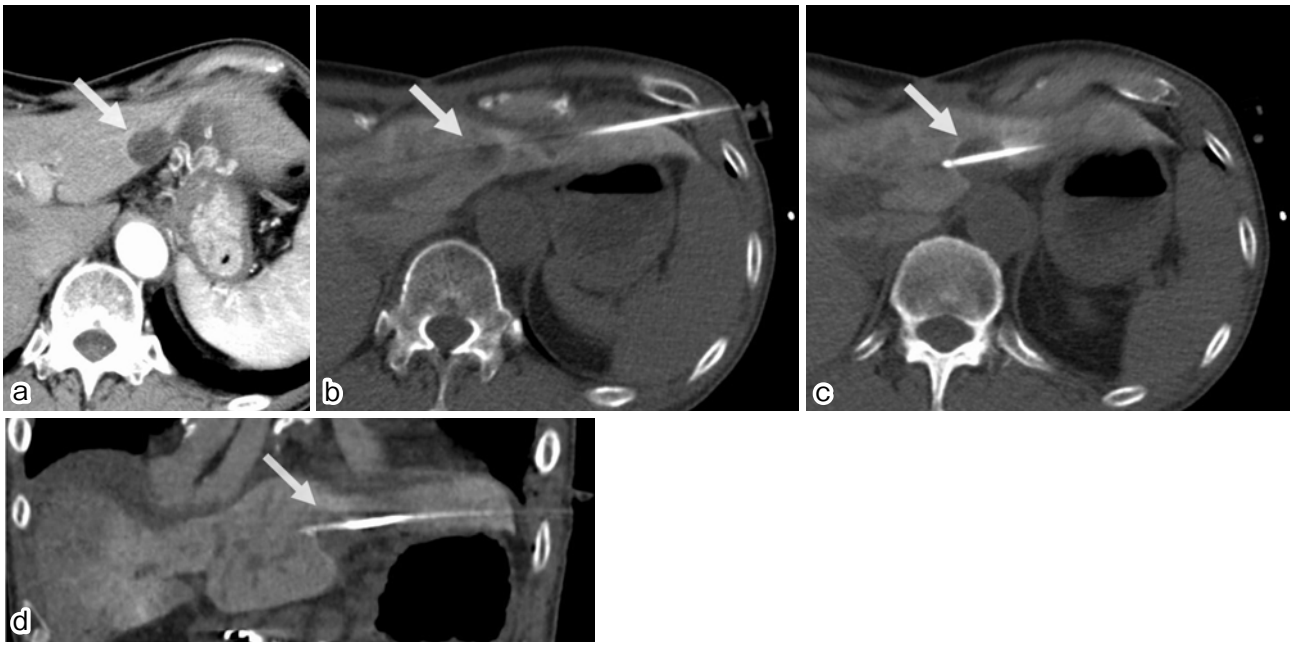

Figure 6. Overlapping ablation of liver metastasis in segment 3 adjacent to adhesive stomach and gastric vessels.
Dynamic enhanced CT reveals metastatic liver tumor at the posterior edge of the segment 3 (a: arrow), adjacent to gastric wall and gastric vessels. The stomach has adhesions due to a previous surgical operation. CT-guided RFA (modified overlapping ablation) is performed for the hypovascular metastatic liver tumor (arrow) from a left intercostal approach, navigating through the thin and long normal liver parenchyma to avoid injury to the adjacent gastric wall. The needle tip is accurately placed within the tumor (b, c). Modified overlapping ablation is performed by adjusting the position of the needle tip at the cranial, center, and caudal regions, respectively. Real-time MPR coronal images are valuable for precise CT-guided RFA (d).

due to the strong adhesion between the liver and the residual stomach following gastric surgery. In this particular case, we performed a CT fluoroscopy-guided puncture using a variable VIVA RF electrode needle (STARmed, Seoul, Korea) after injecting LPD from the left lobe of the liver. This allowed us to perform a "modified overlapping ablation" of the metastatic lesion, which appeared as a low-density area without contrast medium enhancement (**Fig. 6**-**8**) [49].

The puncture technique in this case required simultaneous awareness of the margin in the cephalocaudal direction and the presence of the gastric wall. We referred to multiplanar reconstruction (MPR) images for each puncture. Furthermore, it is worth noting that the tumor was in close proximity to the abdominal aorta during the puncture, necessitating extra caution during the procedure. When performing ablation treatment for metastatic liver cancer, inserting the electrode into a hardened metastatic lesion through the typically soft normal liver tissue requires a keen sense of the needle tip's response to the needle's motion. Even in such cases, it remains crucial to maintain real-time visualization of the needle tip, tumor, and the surrounding structures. In this case, the needle was inserted from three directions: cranial, central, and caudal (**Fig. 7**). It was confirmed that the tumor was ablated with sufficient margin on enhanced CT immediately after the procedure.

RFA of a metastatic tumor in the caudate lobe or deep regions

Caudate lobe lesions are usually considered difficult to puncture due to their anatomical characteristics, and a high rate of local recurrence after RFA has been reported [50, 51]. It remains unclear whether an approach from the right or left hepatic lobe is more effective for percutaneous treatment [52, 53]. This uncertainly further underscores the complexity of addressing caudate lobe lesions.

In this case, securing a suitable puncture line to reach the hypovascular caudate lobe metastases posed a formidable challenge due to the lateral area of the left lobe having been resected in a prior resection and the presence of the stomach anteriorly (**Fig. 7**). To overcome these challenges, we opted for a right intercostal approach, carefully avoiding the stomach by navigating through the remaining thin hepatic parenchyma of the medial segment of the left lobe (S4). This approach involved placing a microcatheter in the proper hepatic artery and puncturing it under the guidance of CT during hepatic arteriography (CTHA) fluoroscopy. This method allowed us to precisely identify the right hepatic artery and establish a secure puncture route with a narrow trajectory (**Fig. 7**). By using a straight-line approach and conducting RFA, we successfully treated the caudate lobe lesion. To ensure comprehensive coverage, we manually inserted a slightly bent electrode slightly dorsal to the tumor's center via the right intercostal space, just above the right branch of the portal vein and in a line just in front of the inferior vena cava. This strategy was employed to achieve a sufficient ablative margin. There were no procedural complications, and the patient is currently under outpatient observation with no evidence of local recurrence 2 years after this treatment.

There are no previous reports of puncture and RFA treatment of liver metastases under CTHA fluoroscopy; thus, it

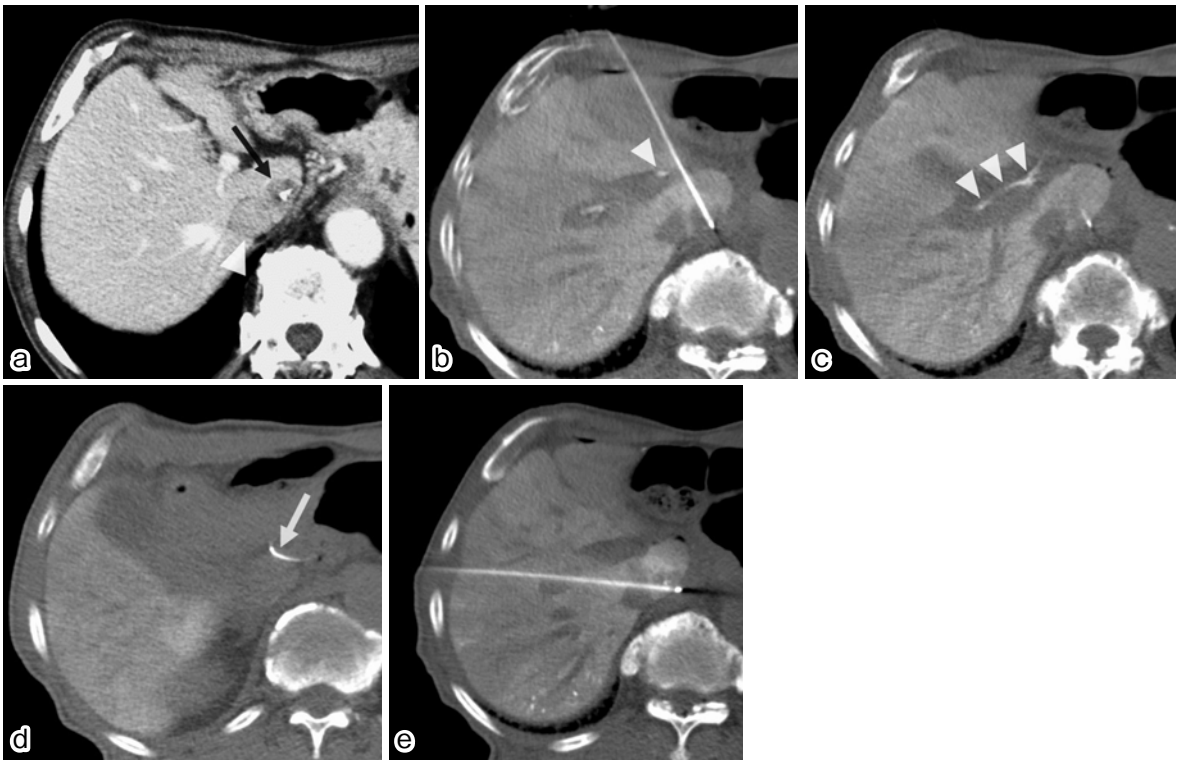

Figure 7. Computed tomography during hepatic arteriography (CTHA)-guided RFA for liver metastasis in caudate lobe.

Enhanced CT reveals a metastatic liver tumor with calcification in caudate lobe (a: arrow), adjacent to the inferior vena cava (IVC) (a: arrowhead). The maximum tumor size measures 15 mm in diameter. The left lateral lobe of the liver has been surgically resected for a previous liver metastasis. CTHA-guided modified overlapping ablation is performed for the hypovascular liver metastasis in the caudate lobe adjacent to IVC. The right hepatic artery is clearly visualized (b, c: arrowhead) near the needle, which was used to puncture the thin normal liver parenchyma of segment 4 from the right hypochondrium approach. A 1.9-Fr microcatheter is shown on CT image (d: arrow). Additional ablation from the right intercostal approach was carried out to ensure a sufficient ablative margin using a curved RF electrode while avoiding injury to the portal vein and IVC (e).

is crucial to accumulate more cases to further refine and evaluate the efficacy of this innovative approach.

RFA for lung metastases adjacent to the aorta or heart

In cases of lung malignant lesions, we perform RFA with a minimum 5 mm ablative margin. For multiple lesions of varying sizes, we use a VIVA RF electrode needle (STARmed, Seoul, Korea) with a length-adjustable active tip [49]. When dealing with lung metastases near critical organs such as large vessels, trachea, bronchus, heart, or pulmonary veins, we routinely use a 1.0 cm or 1.5 cm small active tip to ensure safety around adjacent organs. We employ a "modified overlapping ablation" technique by adjusting the active tip based on tumor size (**Fig. 8**). As with liver tumors, real-time MPR images are generated during treatment to visualize the needle tip from multiple angles.

In addition, we make use of the CT fluoroscopic function with six screens (**Fig. 9**) to enable oblique punctures in the cranio-caudal direction and axial punctures along the body axis (Z-axis). This approach enhances the accuracy and safety of puncturing lesions that are typically challenging. The six-screen CT fluoroscopic function provides instant information about lesions extending in the cranio-caudal direction, making it more advantageous than the conventional three-screen setup.

To manage postoperative pain, especially for lesions near the pleura, a small amount of local anesthetic is occasionally injected between the pleural wall and the visceral side before ablation. Depending on the case, this can help prevent postoperative pain. It is worth noting that there are reported risks associated with these procedures. The risk of brachial plexus injury is 0.5% [15] especially when treating the pulmonary apex (1.3%) [54], and when near the diaphragm, diaphragmatic herniation is reported to be 0.1% [55]. **Fig. 10** shows an example of a challenging case of RFA for pulmonary metastasis. When treating lesions close to the large bronchus, pulmonary vessel, pleura, mediastinum, or pulmonary hilum, it is crucial to obtain informed consent regarding the potential risk of bleeding or nerve disorder should be done. In these challenging cases, it is essential to master basic CT-guided puncture techniques through daily practice.

Challenging Cases of Percutaneous Drainage

Image-guided percutaneous drainage or aspiration of abscesses and abnormal fluid collections are some of the pre-

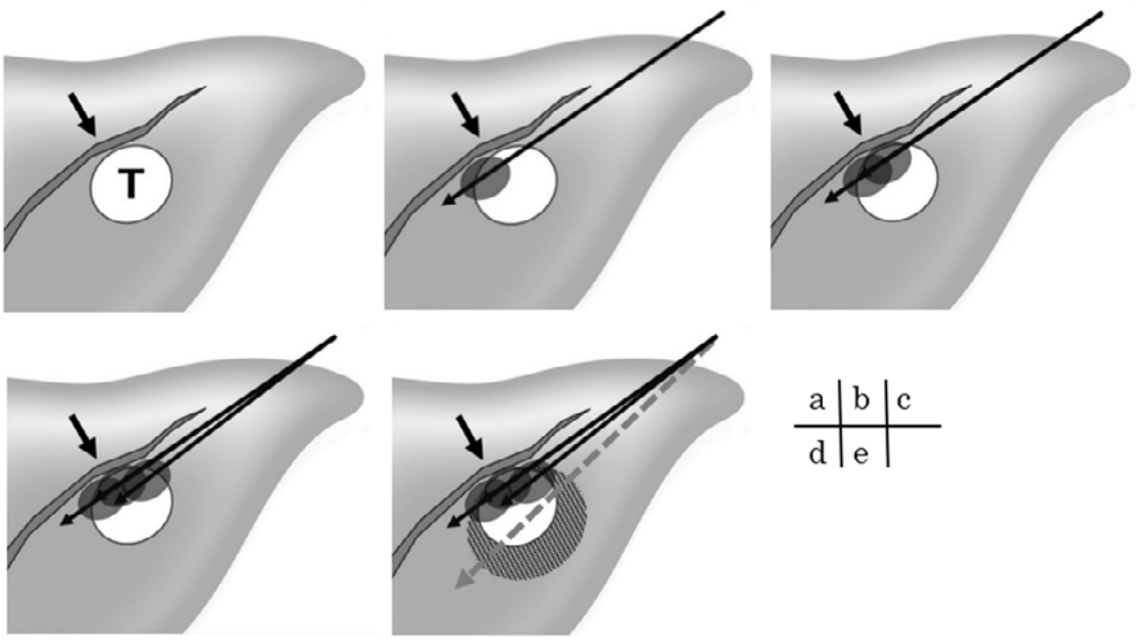

Figure 8. Modified overlapping ablation technique by length-adjustable RF electrode.
a: Target tumor is adjacent to a vessel or a dangerous organ (T: tumor, black arrow: vessel, trachea, gall bladder, or intestine).
b: First, a small area of RFA near the dangerous organ is performed with an adjustable needle with a 1 cm active tip.
c: Second, the proximal lesion near the dangerous organ is ablated.
d: Third, a more proximal lesion near the dangerous organ is ablated by changing the position of the needle tip.
e: Finally, at the distal lesion from the dangerous organ in the target tumor, a safe and wide ablation is performed with a sufficient ablative margin.

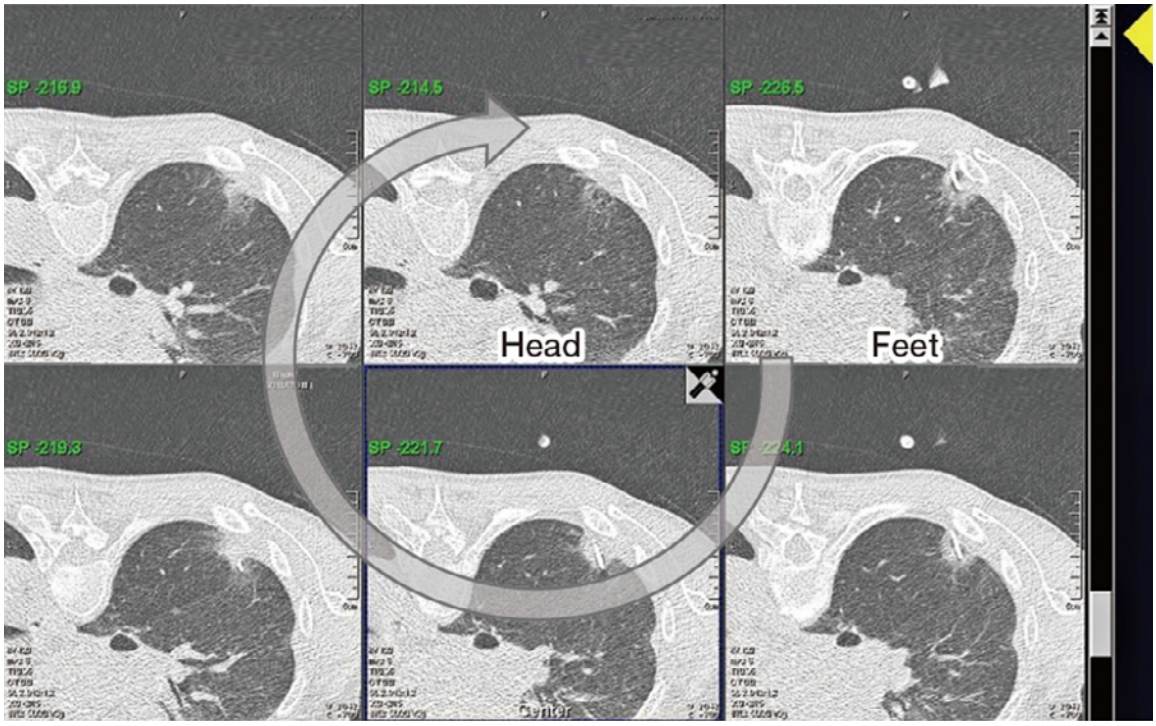

Figure 9. The six real-time different section images are demonstrable at a glance on CT fluoroscopy.
Using the CT fluoroscopic function of six screens, the interventional radiologist can perform an oblique puncture in the cranio-caudal direction and axial puncture in the direction of the body axis (Z-axis), making safe and accurate puncture possible for lesions typically considered challenging to treat. Since information about lesions that extend in the cranio-caudal direction is instantly obtained, the CT fluoroscopic function of six screens proves more useful than the conventional three screens (arrow: Six real-time images are simultaneously displayed in the direction of the arrow from the caudal side to the cranial side of the patient. It is evident that the RFA needle is inserted through the center of the tumor from the caudal side toward the cranial side).

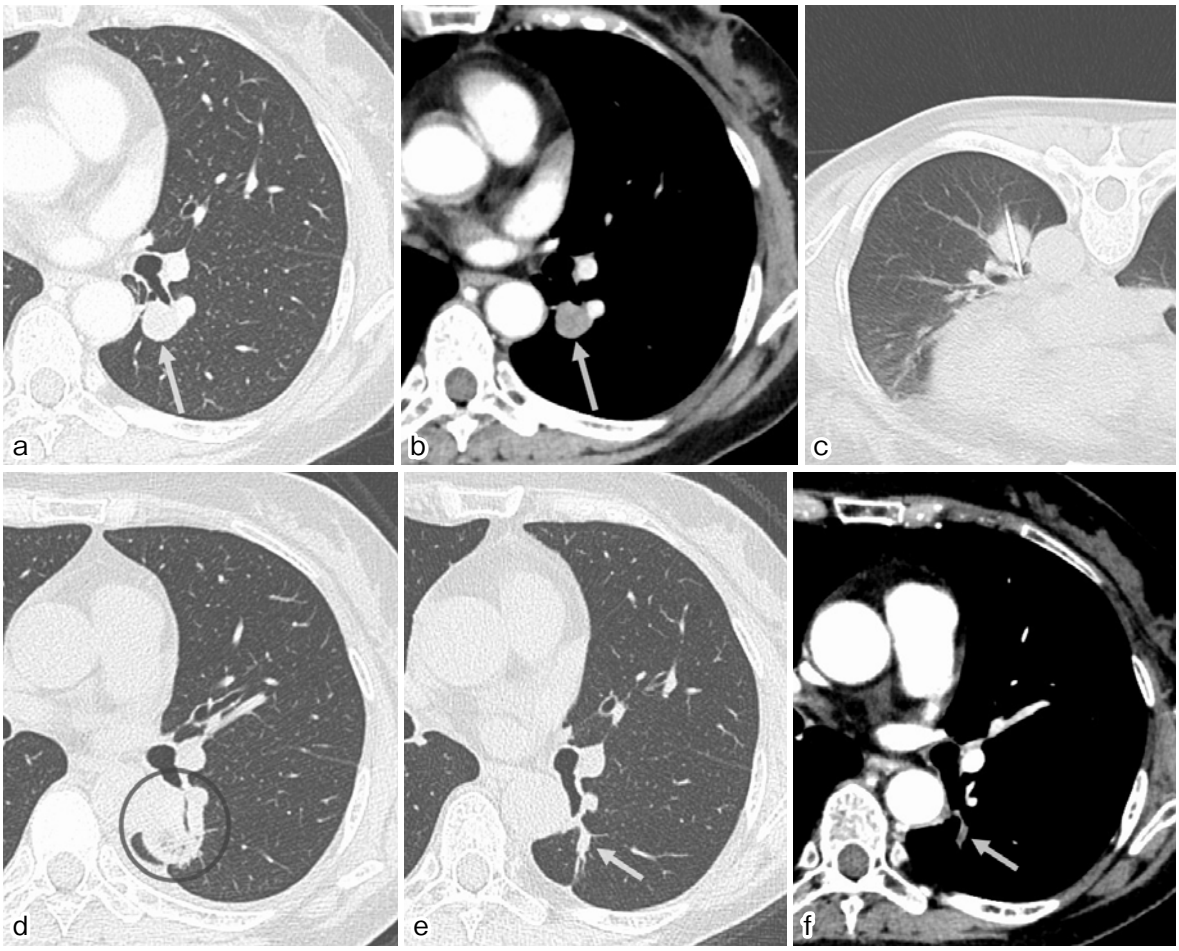

Figure 10. Challenging case of RFA for lung metastasis adjacent to the organ at risk.
The metastatic lung tumor was located in segment 6 of the left lung adjacent to the left lower bronchus and pulmonary vein (a, b: arrow). RFA was performed using a VIVA RF electrode with a 2.5 cm active tip (c). One month after the treatment of the initial ablation (d), ablated area was shown as ground-glass opacity (circle). Two years after the RFA, the ablated area was shown as a scar (e, f: arrow) without injury of the bronchus or pulmonary vein. Additional PET-CT showed no obvious FDG accumulation in the treated area, which was judged as complete response.

ferred diagnostic and therapeutic techniques for a wide range of fluid collections. These procedures have led to reduced morbidity and mortality, as well as shorter hospital stays and lower costs [4]. Percutaneous drainage can sometimes dramatically improve clinical symptoms without the need for medical or surgical intervention. While it is often performed under US guidance, CT-guided puncture drainage is particularly effective in areas where air is present, such as the intestinal tract and lungs, as well as for deep lesions.

Percutaneous drainage of perimediastinal region

Among the various drainages, we focus on a challenging case involving a posterior mediastinal abscess. Puncturing the perimediastinal region requires great care due to the presence of many vital organs nearby. Although there are reports on the use of methods such as the tandem [56], trocar, and Seldinger methods [57], there have been cases of misplacement into the pulmonary vein [57], making puncture a challenge. Puncturing the anterior mediastinum can be done via the sternum or lateral to it. The internal thoracic artery runs laterally, with the vein on the medial side; therefore, particular attention is needed to avoid the internal thoracic artery when puncturing the anterior mediastinum.

Puncturing an abscess in the posterior mediastinum, located ventral to the vertebral body, can be difficult due to the vertebral body and lungs. However, it can be punctured through the fat layer of the vertebral limbus. If the fat layer is this, the puncture path can be extended by injecting local anesthesia or saline solution.

A male patient in his 70s initially presented with a persistent cough and fever. CT scans revealed bilateral pleural effusions. Conservative treatment did not yield satisfactory results, and contrast-enhanced CT revealed fluid accumulation in the posterior mediastinum (anterior thoracic vertebral body) with an unclear contrast effect on the peripheral component, leading to a diagnosis of a posterior mediastinal abscess (**Fig. 11**).

To address this, he was placed in the left lateral decubitus position, and the approach was made from the right intercostal space. However, the right-sided protrusion of the thoracic vertebral body and the curvature of the ribs made a straight puncture difficult. Therefore, we manually bent an

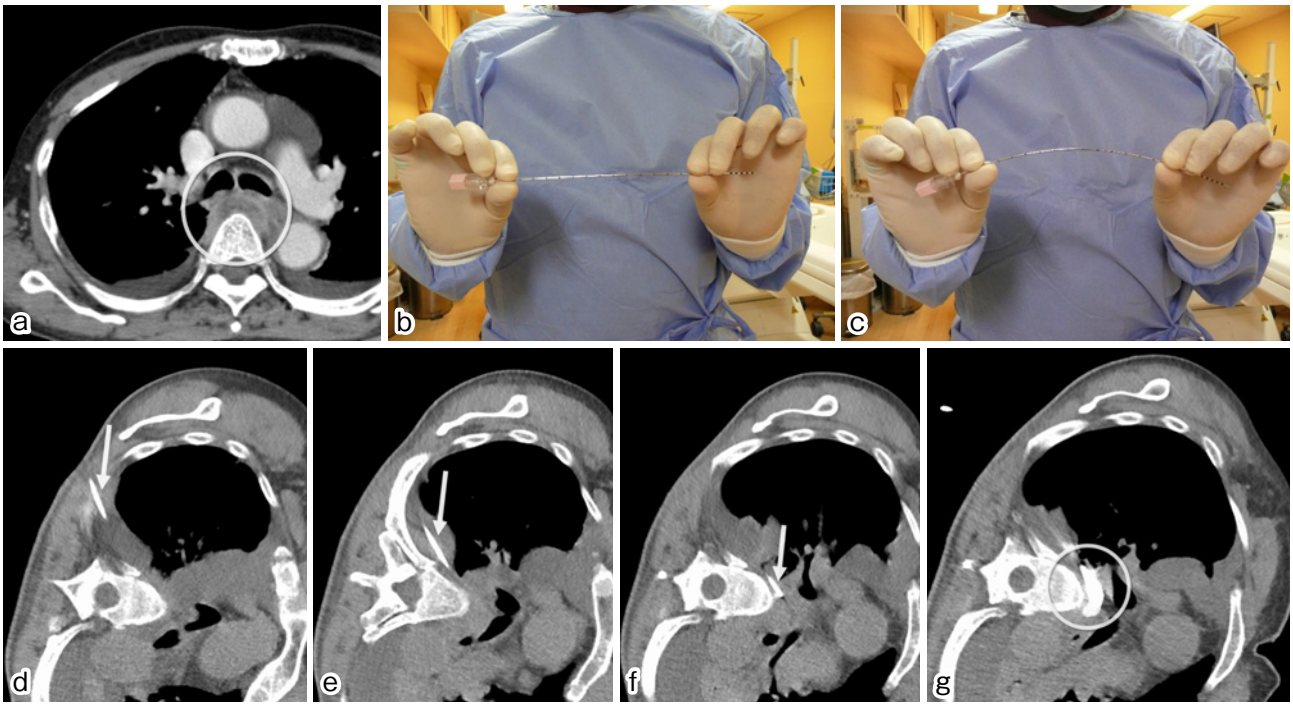

Figure 11. Posterior mediastinal abscess drainage using needle bending manipulation technique.
A posterior mediastinal abscess is revealed as a fluid collection with an enhanced thickened wall adjacent to the trachea and vertebra (a: circle: abscess cavity). Needle bending is performed by hand for the challenging CT-guided puncture (b: before, c: after). CT-guided peri-vertebral puncture through pleural effusion is performed using the bent needle (arrow) for the posterior mediastinal abscess (d–f). A 7-Fr pigtail catheter is inserted into the posterior mediastinal abscess without complications (g) (circle: abscess cavity of the posterior mediastinum delineated by diluted contrast material).

18-G PTBD needle (**Fig. 11**) to create an arc-like safe puncture line. We then percutaneously and transthoracically punctured the posterior mediastinal abscess under CT fluoroscopic guidance, carefully avoiding the surrounding structures (**Fig. 11**). Subsequently, a 7-Fr pigtail catheter was placed over the wire to complete the percutaneous drainage. After approximately 3 weeks of drainage, inflammatory findings improved, the abscess disappeared, and he was discharged from the hospital without drainage tube.

It is worth noting that manual bending of the puncture needle is not recommended by the manufacturer, as excessive bending can cause the internal needle to become stuck and resist guidewire insertion using the Seldinger method. Although there have been reports on the usefulness of steerable needles [58, 59], they are currently off-label in Japan, and we anticipate their approval in the near future.

Conclusions

This article highlights innovations in puncture techniques that enable successful management of challenging cases, with a particular focus on cases that have not been comprehensively reported in previous review articles. Image-guided percutaneous puncture is a procedure commonly performed in various healthcare institutions and organ-specific departments. However, certain cases pose unique challenges. In such instances, the ability of IRists to guide patients effectively and achieve their objectives is of paramount importance, positioning them as leaders within their respective institutions.

Success in these cases hinges on expanding the repertoire of techniques and procedures available for daily practice in percutaneous puncture procedures. In conclusion, we firmly believe that the continued development of image-guided puncture techniques, such as US, fluoroscopy, CT, and CT fluoroscopy, combined with a comprehensive understanding of anatomical structures, will significantly influence treatment decision-making and the quality of patient care.

We hope that this article will serve as a valuable resource for IRists, aiding them in enhancing their proficiency in safe and precise image-guided puncture techniques.

Conflict of Interest: None
Disclaimer: Taku Yasumoto is one of the Editorial Board members of Interventional Radiology. This author was not involved in the peer-review or decision-making process for this paper.

References

1. Sheth RA, Baerlocher MO, Connolly BL, et al. Society of Interventional Radiology quality improvement standards on percutaneous needle biopsy in adult and pediatric patients. J Vasc Interv Radiol. 2020; 31: 1840-1848.
2. Lane BR, Samplaski MK, Herts BR, Zhou M, Novick AC, Campbell SC. Renal mass biopsy—a renaissance? J Urol. 2008; 179: 20-27.

3. Iguchi T, Matsui Y, Tomita K, et al. Computed tomography-guided core needle biopsy for renal tumors: A review. Interv Radiol (Higashimatsuyama). 2021; 6: 69-74.
4. Dariushnia SR, Mitchell JW, Chaudry G, Hogan MJ. Society of Interventional Radiology quality improvement standards for image-guided percutaneous drainage and aspiration of abscesses and fluid collections. J Vasc Interv Radiol. 2020; 31: 662-666.e4.
5. Keeling AN, Leong S, Logan PM, Lee MJ. Empyema and effusion: outcome of image-guided small-bore catheter drainage. Cardiovasc Intervent Radiol. 2008; 31: 135-141.
6. Devane AM, Annam A, Brody L, et al. Society of Interventional Radiology quality improvement standards for percutaneous cholecystostomy and percutaneous transhepatic biliary interventions. J Vasc Interv Radiol. 2020; 31: 1849-1856.
7. Al Mahjoub A, Menahem B, Fohlen A, et al. Preoperative biliary drainage in patients with resectable perihilar cholangiocarcinoma: Is percutaneous transhepatic biliary drainage safer and more effective than endoscopic biliary drainage? A meta-analysis. J Vasc Interv Radiol. 2017; 28: 576-582.
8. Dorcaratto D, Hogan NM, Muñoz E, et al. Is percutaneous transhepatic biliary drainage better than endoscopic drainage in the management of jaundiced patients awaiting pancreaticoduodenectomy? A systematic review and meta-analysis. J Vasc Interv Radiol. 2018; 29: 676-687.
9. Hassan Z, Gadour E. Percutaneous transhepatic cholangiography vs endoscopic ultrasound-guided biliary drainage: a systematic review. World J Gastroenterol. 2022; 28: 3514-3523.
10. Shiina S, Sato K, Tateishi R, et al. Percutaneous ablation for hepatocellular carcinoma: Comparison of various ablation techniques and surgery. Can J Gastroenterol Hepatol. 2018; 2018: 4756147; doi: 10.1155/2018/4756147.
11. Sato Y, Hasegawa T, Chatani S, Murata S, Inaba Y. Percutaneous radiofrequency ablation for liver tumors: Technical tips. Interv Radiol (Higashimatsuyama). 2020; 5: 50-57.
12. Tanis E, Nordlinger B, Mauer M, et al. Local recurrence rates after radiofrequency ablation or resection of colorectal liver metastases. Analysis of the European Organisation for Research and Treatment of Cancer #40004 and #40983. Eur J Cancer. 2014; 50: 912-919.
13. White RR, Avital I, Sofocleous CT et al. Rates and patterns of recurrence for percutaneous radiofrequency ablation and open wedge resection for solitary colorectal liver metastasis. J Gastrointest Surg. 2007; 11: 256-263.
14. Matsui Y, Iguchi T, Tomita K, et al. Radiofrequency ablation for stage I non-small cell lung cancer: An updated review of literature from the last decade. Interv Radiol (Higashimatsuyama). 2020; 5: 43-49.
15. Hiraki T, Gobara H, Fujiwara H, et al. Lung cancer ablation: Complications. Semin Intervent Radiol. 2013; 30: 169-175.
16. Lyons NJR, Pathak S, Daniels IR, Spiers A, Smart NJ. Percutaneous management of pulmonary metastases arising from colorectal cancer; a systematic review. Eur J Surg Oncol. 2015; 41: 1447-1455.
17. Hasegawa T, Takaki H, Kodama H, et al. Three-year survival after radiofrequency ablation for surgically resectable colorectal lung metastases: A prospective multicenter study. Radiology. 2020; 294: 686-695.
18. Ahmed M, Solbiati L, Brace CL, et al. Image-guided tumor ablation: standardization of terminology and reporting criteria—a 10-year update. J Vasc Interv Radiol. 2014; 25: 1691-1705.e4.
19. Nakamura K, Matsumoto K, Inoue C, Matsusue E, Fujii S. Computed tomography-guided lung biopsy: A review of techniques for reducing the incidence of complications. Interv Radiol (Higashimatsuyama). 2021; 6: 83-92.
20. Hasegawa T, Chatani S, Sato Y, et al. Percutaneous image-guide needle biopsy of musculoskeletal tumors: technical tips. Interv Radiol (Higashimatsuyama). 2021; 6: 75-82.
21. Cai YL, Xiong XZ, Lu J, et al. Percutaneous needle aspiration versus catheter drainage in the management of liver abscess: a systematic review and meta-analysis. HPB (Oxford). 2015; 17: 195-201.
22. Bevilacqua A, D'Amuri FV, Pagnini F, et al. Percutaneous needle biopsy of retroperitoneal lesions: technical developments. Acta Biomed. 2019; 90: 62-67.
23. Bourgouin PP, Rodriguez KJ, Fintelmann FJ. Image-guide percutaneous lung needle biopsy: How we do it. Tech Vasc Interv Radiol. 2021; 24: 100770.
24. Gupta S, Henningsen JA, Wallace MJ, et al. Percutaneous biopsy of head and neck lesions with CT guidance: various approaches and relevant anatomic and technical considerations. RadioGraphics. 2007; 27: 371-390.
25. Wallace MJ, Gupta S, Hicks ME. Out-of-plane computed-tomography-guided biopsy using a magnetic-field-based navigation system. Cardiovasc Intervent Radiol. 2006; 29: 108-113.
26. Gupta S, Seaberg K, Wallace MJ, et al. Imaging-guided percutaneous biopsy of mediastinal lesions: different approaches and anatomic considerations. RadioGraphics. 2005; 25: 763-786; discussion 786.
27. Gupta S, Madoff DC, Ahrar K, et al. CT-guided needle biopsy of deep pelvic lesions by extraperitoneal approach through iliopsoas muscle. Cardiovasc Intervent Radiol. 2003; 26: 534-538.
28. Gupta S, Madoff DC. Image-guided percutaneous needle biopsy in cancer diagnosis and staging. Tech Vasc Interv Radiol. 2007; 10: 88-101.
29. Huo YR, Chan MV, Habib AR, Lui I, Ridley L. Pneumothorax rates in CT guided lung biopsies: A comprehensive systematic review and meta-analysis of risk factors. Br J Radiol. 2020; 93: 20190866.
30. Cazzato RL, Garnon J, Shaygi B, et al. Performance of a New Blunt-Tip Coaxial Needle for Percutaneous Biopsy and Drainage of "Hard-To-Reach" Targets. Cardiovasc Intervent Radiol. 2017; 40: 1431-1439.
31. Rigiroli F, Camacho A, Chung A, et al. Safety profile and technical success of narrow window CT-guided percutaneous biopsy with blunt needle approach in the abdomen and pelvis. Eur Radiol. 2023; doi: 10.1007/s00330-023-10231-z.
32. Schnapauff D, Marnitz T, Freyhardt P, et al. CT guided bone biopsy using a battery powered intraosseous device. Cardiovasc Intervent Radiol. 2013; 36: 1405-1410.
33. Wallace AN, Pacheco RA, Vyhmeister R, Tomasian A, Chang RO, Jennings JW. Fluoroscopy-guided intervertebral disc biopsy with a coaxial drill system. Skeletal Radiol. 2016; 45: 273-278.
34. Yasumoto T. Biliary interventional procedures: puncture, stent placement, and troubleshooting. Jpn J Intervent Radiol. 2014; 29: 411-422.
35. Funaki B, Zaleski GX, Straus CA, et al. Percutaneous biliary drainage in patients with nondilated intrahepatic bile ducts. AJR Am J Roentgenol. 1999; 173: 1541-1544.
36. Yasumoto T, Yokoyama S, Nagaike K. Percutaneous transcholecystic metallic stent placement for malignant obstruction of the common bile duct: preliminary clinical evaluation. J Vasc Interv Radiol. 2010; 21: 252-258.
37. Shibata T, Iimuro Y, Ikai I, Hatano E, Yamaoka Y, Konishi J. Percutaneous radiofrequency ablation therapy after intrathoracic saline solution infusion for liver tumor in the hepatic dome. J Vasc Interv Radiol. 2002; 13: 313-315.
38. Kang TW, Rhim H, Lee MW, et al. Radiofrequency ablation for hepatocellular carcinoma abutting the diaphragm: comparison of

effects of thermal protection and therapeutic efficacy. AJR Am J Roentgenol. 2011; 196: 907-913.

39. Hasegawa T, Takaki H, Miyagi H, et al. Hyaluronic acid gel injection to prevent thermal injury of adjacent gastrointestinal tract during percutaneous liver radiofrequency ablation. Cardiovasc Intervent Radiol. 2013; 36: 1144-1146.

40. Schlappa M, Wüst W, Siebler J, Grützmann R, Uder M, Schmid A. Efficacy and safety of angioplasty balloon interposition in CT-guided percutaneous thermal ablation of hepatic malignancies to protect adjacent organs. Cardiovasc Intervent Radiol. 2022; 45: 1401-1407.

41. Mulier S, Ni Y, Jamart J, Ruers T, Marchal G, Michel L. Local recurrence after hepatic radiofrequency coagulation: multivariate meta-analysis and review of contributing factors. Ann Surg. 2005; 242: 158-171.

42. Veltri A, Sacchetto P, Tosetti I, Pagano E, Fava C, Gandini G. Radiofrequency ablation of colorectal liver metastases: small size favorably predicts technique effectiveness and survival. Cardiovasc Intervent Radiol. 2008; 31: 948-956.

43. Solbiati L, Ahmed M, Cova L, Ierace T, Brioschi M, Goldberg SN. Small liver colorectal metastases treated with percutaneous radiofrequency ablation: local response rate and long-term survival with up to 10-year follow-up. Radiology. 2012; 265: 958-968.

44. Hamada A, Yamakado K, Nakatsuka A, et al. Radiofrequency ablation for colorectal liver metastases: prognostic factors in non-surgical candidates. Jpn J Radiol. 2012; 30: 567-574.

45. Wang X, Sofocleous CT, Erinjeri JP, et al. Margin size is an independent predictor of local tumor progression after ablation of colon cancer liver metastases. Cardiovasc Intervent Radiol. 2013; 36: 166-175.

46. Yamakado K, Inaba Y, Sato Y, et al. Radiofrequency ablation combined with hepatic arterial chemoembolization using degradable starch microsphere mixed with Mitomycin C for the treatment of liver metastasis from colorectal cancer: A prospective multicenter study. Cardiovasc Intervent Radiol. 2017; 40: 560-567.

47. Yasumoto T, Yakushiji H, Ohira R, et al. Liver metastasis in a gastric cancer patient - A case of successful radiofrequency ablation combined with degradable starch microspheres transcatheter arterial chemoembolization. Gan To Kagaku Ryoho. 2015; 42: 1611-1613.

48. Yasumoto T, Uemoto K, Yamada K, et al. Radiofrequency ablation under computed tomography during arterial portography for hypovascular liver metastases from advanced pancreatic cancer. Gan To Kagaku Ryoho. 2018; 45: 371-373.

49. Yasumoto T, Uemoto K, Yamada K, et al. Radiofrequency ablation of malignant tumors with length-adjustable electrodes. Jpn J Intervent Radiol. 2018; 33: 32-42.

50. Peng ZW, Liang HH, Chen MS, et al. Percutaneous radiofrequency ablation for the treatment of hepatocellular carcinoma in the caudate lobe. Eur J Surg Oncol. 2008; 34: 166-172.

51. Thanos L, Mylona S, Galani P, Pomoni M, Pomoni A, Koskinas I. Overcoming the heat-sink phenomenon: Successful radiofrequency thermal ablation of liver tumors in contact with blood vessels. Diagn Interv Radiol. 2008; 14: 51-56.

52. Dong J, Li W, Zeng Q, et al. CT-guided percutaneous step-by-Step radiofrequency ablation for the treatment of carcinoma in the caudate lobe. Med (Baltim). 2015; 94: e1594.

53. Kariyama K, Nouso K, Wakuta A, et al. Percutaneous radiofrequency ablation for treatment of hepatocellular carcinoma in the caudate lobe. AJR Am J Roentgenol. 2011; 197: W571-W575.

54. Hiraki T, Gobara H, Mimura H, et al. Brachial nerve injury caused by percutaneous radiofrequency ablation of apical lung cancer: a report of four cases. J Vasc Interv Radiol. 2010; 21: 1129-1133.

55. Matsui Y, Hiraki T, Gobara H, et al. Phrenic nerve injury after radiofrequency ablation of lung tumors: retrospective evaluation of the incidence and risk factors. J Vasc Interv Radiol. 2012; 23: 780-785.

56. Tanaka T, Inaba Y, Arai Y, Matsueda K, Aramaki T, Dendo S. Mediastinal abscess successfully treated by percutaneous drainage using a unified CT and fluoroscopy system. Br J Radiol. 2002; 75: 470-473.

57. Arellano RS, Gervais DA, Mueller PR. Computed tomography-guided drainage of mediastinal abscesses: clinical experience with 23 patients. J Vasc Interv Radiol. 2011; 22: 673-677.

58. Rutigliano S, Abraham JA, Kenneally BE, Zoga AC, Nevalainen M, Roedl JB. Analysis of a steerable needle for fine needle aspiration and biopsy: efficiency and radiation dose compared with a conventional straight needle. J Comput Assist Tomogr. 2017; 41: 957-961.

59. De Filippo M, Saba L, Rossi E, et al. Curved needles in CT-guided fine needle biopsies of abdominal and retroperitoneal small lesions. Cardiovasc Intervent Radiol. 2015; 38: 1611-1616.